Published in final edited form as:
Cancer Res. 2011 December 15; 71(24): . doi:10.1158/0008-5472.CAN-11-1714.

GLIPR1 Suppresses Prostate Cancer Development through Targeted Oncoprotein Destruction

Likun Li[1], **Chengzhen Ren**[1], **Guang Yang**[1], **Elmoataz Abdel Fattah**[2,8], **Alexei A. Goltsov**[1], **Soo Mi Kim**[3,9], **Ju-Seog Lee**[3], **Sanghee Park**[1], **Francesco J. Demayo**[4], **Michael M. Ittmann**[5,6], **Patricia Troncoso**[7], and **Timothy C. Thompson**[1,*]

[1]Department of Genitourinary Medical Oncology, Unit 18-3, The University of Texas MD Anderson Cancer Center, Houston, TX 77030, USA

[2]Scott Department of Urology, Baylor College of Medicine, Houston, TX 77030, USA

[3]Department of Systems Biology, Unit 950, The University of Texas MD Anderson Cancer Center, Houston, TX 77030, USA

[4]Department of Molecular and Cellular Biology, Baylor College of Medicine, Houston, TX 77030, USA

[5]Department of Pathology, Baylor College of Medicine, Houston, TX 77030, USA

[6]Michael E. DeBakey Veterans Affairs Medical Center, Houston, TX 77030, USA

[7]Department of Pathology, Unit 85, The University of Texas MD Anderson Cancer Center, Houston, TX 77030, USA

Abstract

Downregulation of the proapoptotic p53 target gene *GLIPR1* occurs frequently in prostate cancer (PCa), but the functional meaning of this event is obscure. Here we report the discovery of functional relationship between GLIPR1 and c-Myc in PCa where c-Myc is often upregulated. We found that the expression of GLIPR1 and c-Myc were inversely correlated in human PCa. Restoration of GLIPR1 expression in PCa cells downregulated c-myc levels, inhibiting cell cycle progression. Downregulation was linked to a reduction in β-catenin/TCF4-mediated transcription of the c-myc gene, which were caused by GLIPR1-mediated redistribution of casein kinase 1α (CK1α) from the Golgi apparatus to the cytoplasm where CK1α could phosphorylate β-catenin and mediate its destruction. In parallel, GLIPR1 also promoted c-Myc protein ubiquitination and degradation by glycogen synthase kinase-3α- and/or CK1α-mediated c-Myc phosphorylation. Notably, genetic ablation of the mouse homolog of *Glipr1* cooperated with c-myc overexpression to induce prostatic intraepithelial neoplasia (PIN) and PCa. Together, our findings provide evidence for CK1α-mediated destruction of c-Myc and identify c-Myc S252 as a crucial CK1α phosphorylation site for c-Myc degradation. Further, they reveal parallel mechanisms of c-myc downregulation by GLIPR1 that when ablated in the prostate are sufficient to drive c-Myc expression and malignant development.

[*]Correspondence: Dr. Timothy C. Thompson, Department of Genitourinary Medical Oncology – Research, Unit 18-3, The University of Texas MD Anderson Cancer Center, 1515 Holcombe Blvd., Houston, TX 77030, USA. timthomp@mdanderson.org; Tel: (713) 792-9955; Fax: (713) 792-9956.
[8]Current address: Department of Medicine, Baylor College of Medicine, Houston, TX, 77030, USA
[9]Current address: Department of Physiology, Chonbuk National University Medical School, Jeonju 561-181, South Korea

Conflict-of-interest statement: The authors have declared that no conflict of interest exists.

Keywords

GLIPR1; c-Myc; CK1α; oncoprotein destruction; prostate cancer

Introduction

Human glioma pathogenesis-related protein 1 (*GLIPR1*) and its mouse counterpart, *Glipr1* are downregulated in prostate cancer (PCa) and other malignant cell lines (1, 2), owing partly to methylation in the gene's regulatory region (3). Loss of *Glipr1* function predisposed mice to tumorigenesis (1). Restoration of GLIPR1 expression in prostate cancer cells and other malignant cells led to growth suppression and/or apoptosis (1–4). Furthermore, a novel *Glipr1* gene–modified tumor cell vaccine had significant antitumor activity in a mouse model of recurrent PCa (5). These preclinical results led to a clinical trial in which PCa patients received a neoadjuvant adenoviral vector–mediated *GLIPR1* injection before undergoing radical prostatectomy. GLIPR1 tumor suppressor activities were also found in two other malignancies: deletion of chromosome region 12q13-24, which contains *GLIPR1* and *GLIPR1*-like genes (6), was found in 34 of 47 colorectal cancer tissues (7), and *GLIPR*1 was deleted in 9% of multiple myeloma patients (8).

In contrast to GLIPR1's tumor suppressor activities in PCa, in glioblastomas, GLIPR1 was upregulated and promoted cell growth, survival, and invasion, suggesting a context-specific role for GLIPR1 in malignant growth (9).

c-MYC is one of the most frequently deregulated genes in cancer [reviewed in (10–12)]. In malignant cells, deregulated c-Myc expression occurs via many mechanisms, including transactivation by certain transcriptional factors, and stabilization of c-Myc mRNA and protein (11, 12) (13, 14). Recent studies identified a complex signaling pathway that controls c-Myc protein stability, involving reversible phosphorylation at threonine 58 (T58) and serine 62 (S62) of c-Myc and Fbw7-mediated ubiquitination and proteasome degradation (15–21). Interestingly, casein kinase 1 (CK1) was recently reported to be involved in ubiquitination and proteasome degradation of dMyc in *Drosophila* (22). Since functional conservation of c-Myc and dMyc was demonstrated in several experimental systems (23), CK1's regulation of dMyc protein stability in *Drosophila* raises the question whether CK1 also has a role in regulating c-Myc protein stability in mammals.

GSK3β and CK1α are members of the serine/threonine-specific protein kinase family. In many cases, GSK3β phosphorylation marks target proteins for ubiquitination and proteolysis (24, 25). GSK3β phosphorylation of c-Myc creates a recognition motif for E3 ubiquitin ligase Fbw7, leading to subsequent ubiquitination and proteasome-mediated c-Myc degradation. In the canonical Wnt signaling pathway, GSK3β phosphorylation of β-catenin promotes proteasomal targeting and degradation of β-catenin (24–26). GSK-3β phosphorylation is also implicated in ubquitination and destruction of several other important signaling molecules, such as HIF-1α, NFκB, cyclins D1 and E, and Cdc25A [reviewed in (24)]

Like GSK3β, CK1 is implicated in ubiquitination and degradation of several important signaling molecules. In the canonical Wnt signaling pathway, CK1α phosphorylates β-catenin at S45, priming for subsequent phosphorylation of β-catenin at T41, S37, and S33 by GSK3β and leading to proteasomal targeting and degradation of β-catenin (27–30). CK1α is also involved in proteasomal degradation of Ci-155 in Hedgehog signaling (28, 31).

To explore the prospect of using GLIPR1 as a potential therapeutic agent for PCa and other cancers in which c-myc is upregulated, we studied the functional relationship between

GLIPR1 and c-Myc in PCa, focusing on GLIPR1's regulation of c-Myc, the synergistic effects of *Glipr1* loss and c-Myc overexpression on tumorigenesis in experimental mouse models, and the mechanisms involved in GLIPR1-induced c-Myc downregulation.

Materials and Methods

Cell lines and cell culture

LNCaP, VCaP, DU145, PC-3 and TSU-Pr1 were from ATCC. R24 is a GLIPR1-inducible stable clone derived from TSU-Pr1 (1). LAPC4 was a gift from Dr. Charles Sawyers of the University of California at Los Angeles and was 293 PE was obtained from Dr. Margaret Goodell of Baylor College of Medicine. Cell lines were validated by STR DNA fingerprinting using the AmpF STR Identifiler kit in the MDACC Cell Line Core.

Cell synchronization and serum restimulation

After adenoviral vector-mediated gene transduction or cDNA transfection, cells were grown in complete medium for 24 h, synchronized by serum starvation for 24 h, and then restimulated by the addition of 10% FBS for 30 min.

Quantitative RT-PCR

Quantitative RT-PCR was performed as described previously (1) using specific Taqman probes and primers (see Supplemental Materials and Methods). In the 34 specimens used for GLIPR1 and c-myc mRNA expression correlation analysis, there were 3 pT1, 27 pT2, and 4 pT3 cancers, with Gleason scores of 6 (n=17), 7 (n=16), and 8 (n=1).

cDNA microarray analysis

Total RNA was isolated from LNCaP, VCaP, and DU145 PCa cell lines. cDNA microarray analysis was performed, and the data were normalized and statistical analysis performed as previously described (32). Microarray data were deposited in GEO database (accession number: GSE32367).

Western blotting analysis

Antibodies: GLIPR1 (described previously (2)); c-Myc, CK1α, and CK1δ (Santa Cruz); active β-catenin (Millipore); P-c-Myc (T58), P-c-Myc (S62) and fibrillarin (Abcam); GSK-3β, P-GSK-3β (S9), β-catenin (total), P-β-catenin (S45), P-β-catenin (T41/S45) and P-β-catenin (S33/S37/T41) (Cell Signaling); β-actin (Sigma). Quantitative analysis was performed -using computer-assisted densitometry, in which total protein was normalized with β-actin and phosphorylated protein was normalized by its total protein. The fraction of phosphorylated protein in control cells was set as 1.

Generation of PB-c-myc;*Glipr1* bigenic mice

We intercrossed founder hemizygous PB-c-myc mice (Supplemental Materials and Methods) with $Glipr1^{+/+}$ or $Glipr1^{-/-}$ mice and bred these mice to generate the following four genotypes: PB-c-myc$^{(+)}$;$Glipr1^{+/+}$, PB-c-myc$^{(+)}$;$Glipr1^{-/-}$, PB-c-myc$^{(-)}$;$Glipr1^{+/+}$, and PB-c-myc$^{(-)}$;$Glipr1^{-/-}$. The resulting male bigenic mice were euthanized when they were approximately 1 year old or when they displayed signs of distress or became moribund.

Immunohistochemistry

Twenty radical prostatectomy specimens which had a pathological differentiation pattern of Gleason score 6 and a pathological stage of pT2b were used for correlative analysis of c-Myc and GLIPR1. GLIPR-1 immunostaining was scored according to the staining intensity

ranging from 0 (negative) to 3 (strong) and the extent of positive staining of the cancerous area (1 = < 10%; 2 = 10–50%; 3 = > 50%). c-Myc immunostaining was measured quantitatively by a Nikon Eclipse 90i system with NIS-element AR software (version 3.0); the results were recorded as the c-Myc–nuclear area ratio of cancer cells (33).

Immunofluorescence

Immunofluorescence was evaluated by using a Nikon Eclipse 90i system with NIS-Elements AR software (version 3.0). To evaluate the cellular distribution of CK1α, a *Z* series of optical sections (0.10-μm steps) was digitally imaged and deconvolved by using AutoQuant deconvolution software (Media Cybernetics) to generate high-resolution images.

Chromatin immunoprecipitation assay

ChIP assays were performed by using a Millipore ChIP kit. The input and immunoprecipitated DNAs were subjected to PCR using primers corresponding to the −718 to −460 base pairs upstream of the c-myc transcription start site (upper primer: 5′CTCAGTCTGGGTGGAAGGTA3′; lower primer: 5′CAGGGAGAGTGGAGGAAAGA3′). Antibodies: TCF4 (Santa Cruz), trimethyl-histone H3K4 (ab8580, Abcam), trimethyl-histone H3K27 (, Millipore), acetyl-histone H3K27 (Millipore) RNA polymerase II (Sigma) and normal rabbit IgG (Santa Cruz).

Promoter construction and luciferase assay

The c-myc promoter (1,316 bp) was amplified by PCR using genomic DNA from normal prostate tissue (see Supplement Materials and Methods). The purified PCR product was phosphorylated and then cloned to pGL3-Basic vector (Promega) using the SmaI site to generate c-myc-luc. Luciferase assay was performed as described previously (1).

c-Myc ubiquitination analysis

The 293 cells were transfected with HA-ubiquitin (Addgene), c-myc, and GLIPR1 or control vector pcDNA. Cells were grown in complete medium for 24 h and synchronized by incubation in serum-free medium (SFM) for 24 h; GM132 was added in the last 4 h of incubation in SFM. Immunoprecipitation was performed with an ubiquitin monoclonal antibody (Sigma).

c-Myc phosphorylation mutants

c-Myc T58A, S67A, and S252A point mutations were each introduced by two-round PCR (Phusion High-Fidelity PCR kit, New England BioLabs). See Supplemental Materials and Methods for details.

Protein stability analysis

DU145 cells were transfected with WT or mutant c-myc. Cells were grown in complete medium for 48 h and then treated with cycloheximide (100 μg/ml) in SFM for the indicated time. After western blotting, c-Myc protein band was measured by computer-assisted densitometry, and the half-life was determined by linear fitting the densitometry data.

Statistical analysis

Paired *t* testing was used for statistical comparisons of GLIPR1 and c-myc mRNA expression in normal and malignant human prostate tissues, and unpaired *t* testing was used in other experiments in which probability was determined. Spearman’s rank-order correlation coefficient test was applied to GLIPR1 and c-myc mRNA levels, to GLIPR1

methylation and c-myc mRNA expression and to GLIPR-1 and c-Myc nuclear immunostaining scores on human PCa specimens.

Results

GLIPR1 and c-Myc expression are inversely correlated in human prostate cancer tissue

To identify a possible functional relationship between GLIPR1 and c-Myc in human PCa, we performed quantitative reverse-transcription (qRT)-PCR comparing 34 human PCa tissue samples and their paired adjacent normal prostate tissue samples. GLIPR1 was downregulated in 27 of the 34 PCa samples relative to the corresponding adjacent normal prostate tissue. In contrast, c-Myc was upregulated in 29 of the 34 PCa tissue samples (Fig. 1A and 1B). Overall, GLIPR1 mRNA expression was significantly lower and c-myc mRNA expression, significantly higher in the PCa tissue samples than in the normal prostate tissue samples (inserts in Fig. 1A and 1B). Spearman's rank-order correlation analysis revealed an inverse correlation between GLIPR1 mRNA expression and c-myc mRNA expression (Fig. 1C). Using our previous GLIPR1 methylation data (3) from 11 pairs of human PCa patient tissue samples that overlapped with 34 pairs of human PCa patient tissue samples used in this study, we found that *GLIPR1* methylation is significantly positively correlated to c-myc mRNA expression (Fig. 1D).

In 20 human prostate cancer radical prostatectomy specimens with a pathological differentiation pattern of Gleason score 6 and a pathological stage of pT2b, immunostaining of GLIPR1 and c-Myc immunostainings showed generally decreased GLIPR1 and increased c-Myc protein expression in the human PCa cells relative to that in the normal prostate epithelial cells (Fig. 1E), a result consistent with previous reports (2, 34). Correlation analysis of the immunostaining results revealed inversely correlated GLIPR1 and c-Myc protein levels (Fig. 1F).

Restoring GLIPR1 expression in prostate cancer cells leads to downregulation of c-Myc and cell cycle inhibition

To assess the global functions of GLIPR1 and the functional relationship between GLIPR1 and c-myc in PCa, we performed comparative cDNA microarray analysis on samples from GLIPR1-transduced LNCaP, VCaP, and DU145 PCa cell lines that express low or undetectable GLIPR1. In addition to changes in the genes involved in cell survival, apoptosis, and redox balance (Fig. S1A), we found that restoring GLIPR1 expression in PCa cells led to changes in expression of c-myc and multiple c-myc downstream target genes, including downregulation of several cell cycle–promoting molecules, such as cyclins A2, B1, B2, and D1 and CDC25C, and upregulation of the cell cycle suppressor p21 (Fig. 2A). We confirmed these microarray results by qRT-PCR (Fig. S1B) and at the protein level by western blotting (Fig. 2B).

To assess the biological effects of downregulation of c-myc and cell cycle–related c-myc target genes, we conducted cell cycle analysis with propidium iodide staining and flow cytometry. Restoration of GLIPR1 expression in LNCaP and DU145 PCa cells reduced the cells in the S phase and substantially increased those in G2 (Fig. 2C and 2D). Results in VCaP and PC-3 cells were similar (Fig. S1C). Interestingly, in LAPC4 cells, instead of cell increase in G2, a markedly increased cell population was found in post G2/M (Fig. S1C). A substantial increase in sub-G1 phase cells was also induced after GLIPR1 expression in LNCaP, VCaP and LAPC4 cells (Fig. 2C, 2D and Fig S1C), which may indicate GLIPR1-induced cell death as we reported previously (1, 2).

Loss of Glipr1 and overexpression of c-myc have synergistic effects

To gain insight into the possible synergism between GLIPR1 loss and c-Myc overexpression in prostatic neoplasia in vivo, we bred PB-cmyc^{+} mice with *Glipr1*$^{+/+}$ or *Glipr1*$^{-/-}$ mice (see Supplemental Materials and Methods) and analyzed prostate tissues of the bigenic mice. As summarized in Table 1 and shown in Fig. 3A–I, no malignant phenotype was found in WT mice. Loss of *Glipr1* alone or overexpression of PB-c-myc alone induced epithelial hyperplasia with atypia and mPIN, but not PCa. However, *Glipr1* loss plus PB-c-myc overexpression significantly increased mPIN lesions and induced locally invasive carcinomas. These carcinomas developed in dorsolateral (n=3) and ventral (n=1) prostates of the bigenic mice (Fig. 3). Three of them had a size >1 mm and extend into the periprostatic loose connective tissues. Another carcinoma protruded into the desmoplastic periglandular stroma. The nuclei of both the mPIN cells and the cancer cells were strongly labeled by AR antibody (Fig. S2A–D), but not by IgG (Fig. S2E) or synaptophysin antibody (Fig. S3A–B), a biomarker for the neuroendocrine (Fig. S3C). PCNA- and TUNEL-positive cells were found both in epithelial atypia of PB-c-myc^{+};*Glipr1*$^{+/+}$ (Fig. 3D and G) and in mPIN lesions of PB-c-myc^{+};*Glipr1*$^{-/-}$ mice (Fig. 3E and H). Interestingly, the proliferative activity in PCa of PB-c-myc^{+};*Glipr1*$^{-/-}$ was remarkably increased and its apoptotic activity was relatively low (Fig. 3F and I). In addition, cMyc immunostaining was stronger in mPIN of PB-c-myc^{+};*Glipr1*$^{-/-}$ (Fig. 3L) than that in the mPIN of PB-c-myc^{+};*Glipr1*$^{+/+}$ mice (Fig. 3K). These in vivo data strongly demonstrate the synergistic effects of *Glipr1* function loss and PB-c-myc overexpression.

GLIPR1 negatively regulates c-myc promoter activities

To elucidate the mechanisms by which GLIPR1 regulates c-myc expression, we assessed the changes in c-myc mRNA in response to changes in GLIPR1 expression in PCa cells. Restoring GLIPR1 in PCa cells in which GLIPR1 was downregulated led to reduced c-myc mRNA levels in all five PCa cell lines tested (Fig. 4A). Conversely, knockdown of endogenous GLIPR1 expression with GLIPR1-specific siRNA led to increased c-myc mRNA expression in PC-3 and R24 (a GLIPR1-inducible clone generated from TSU-Pr1 bladder cancer cells), both of which express moderate GLIPR1 levels (Fig. 4B).

Since c-myc mRNA levels are inversely related to GLIPR1 expression, we next asked whether GLIPR1 regulates *c-MYC* transcription. As *c-MYC* is an important downstream target of Wnt-β-catenin signaling (13, 35), we speculated that GLIPR1 facilitates *c-MYC* downregulation by disrupting β-catenin signaling. Western blotting revealed downregulation of β-catenin after enforced GLIPR1 expression in PCa cells (Fig. 4C). Subcellular fractionation analysis further showed that GLIPR1 expression substantially decreases active β-catenin in both cytoplasolic and nuclear cellular fractions (Fig. 4D).

To obtain direct evidence of GLIPR1's regulation of *c-MYC* transcription, we performed both chromatin immunoprecipitation (ChIP) analysis and luciferase promoter assays in GLIPR1-expressing or control lacZ–expressing PCa cells. ChIP results showed that enforced expression of GLIPR1 in DU145 cells led to increased H3K27 trimethylase mark and reduced the pol II, H3K4 trimethylase and H3 acetylase marks on the *c-MYC* promoter indicating diminished transactivation activities (Fig. 4E). Importantly, GLIPR1 expression led to reduced *c-myc* promoter binding to TCF4, the DNA binding protein that mediates β-catenin transcriptional regulation, by more than 3-fold (Fig. 4E). The reduced TCF4 binding to *c-MYC* promoter together with reduced nuclear active β-catenin (Fig. 4D) indicate diminished *c-MYC* transcription. We also confirmed that GLIPR1 suppresses *c-MYC* transcriptional activity by using c-myc–luciferase promoter assays in PC-3M PCa cells (Fig. 4F).

Since GSK3β and CK1α are involved in the destruction of β-catenin, we examined GSK3β and CK1α expression and distribution in GLIPR1-expressing PCa cells. GSK3β levels were slightly increased in GLIPR1-transduced DU145 cells (Figs. 4G and S4A), whereas CK1α protein levels were remarkably higher in GLIPR1-transduced PCa cells (Figs. 4G and S4B) and inversely correlated with β-catenin and c-Myc protein levels (Figs. 4C, 4D and S4A). These results are consistent with the results of our cDNA microarray experiments (Fig. S5). Interestingly, restoring GLIPR1 expression in PCa cells also led to marked redistribution of CK1α. In control lacZ-expressing cells, CK1α is predominantly localized in the perinuclear region within or near the Golgi complex, but in GLIPR1-expressing cells, CK1α spreads out from Golgi to cytoplasm (Fig. 4H), where it can potentially be recruited to the β-catenin destruction complex and facilitate β-catenin's phosphorylation. Indeed, the fraction of phosphorylated β-catenin at S45 in total β-catenin was ~3.8-fold higher in GLIPR1-expressing cells compared with lacZ control cells (Fig. 4I). This crucial priming phosphorylation led to remarkably increased subsequential phophorylation of β-catenin at T41, S37 and S33 (Fig. 4I). These results show that GLIPR1 promotes β-catenin destruction, which in turn leads to suppressed c-myc transcription.

CK1α is crucial in GLIPR1-induced c-Myc protein ubiquitination and proteasome degradation in prostate cancer cells

Although our results showed that GLIPR1 downregulates both c-myc mRNA and protein, the GLIPR1-stimulated reductions in c-myc mRNA levels were limited to ~50% (Fig. 4A), whereas the reductions in c-Myc protein ranged from 3- to 10-fold (Figs. 2B, 4C, and 4G). We thus asked whether GLIPR1 regulates c-Myc protein stability in addition to its regulation of c-myc transcription. To answer this question, we cotransfected the 293 cells with GLIPR1 or control vector pcDNA together with c-myc and ubiquitin, and performed immunoprecipitation and western blotting analysis for ubiquitinated c-Myc. We found that GLIPR1 expression led to a definitive increase of ubiquitinated c-Myc (Fig. 5A). Three different proteasome inhibitors maintained c-Myc levels in the presence of GLIPR1 levels that effectively suppressed c-Myc in all four cell lines tested (Fig. 5B and Fig. S6). Thus, our results demonstrated that GLIPR1-induced c-Myc downregulation involves c-Myc protein ubiquitination- and proteasome-mediated degradation.

We next addressed the mechanisms by which GLIPR1 facilitates these actions. We examined c-Myc phosphorylation at T58 and the priming phosphorylation at S62. In DU145 cells, GLIPR1 expression led to decreased c-Myc total protein by ~3-fold compared with lacZ control. The fraction of phosphorylated c-Myc at T58 in total c-Myc increased ~6.6-fold and that at S62 increased ~3.2-fold in GLIPR1 overexpressed cells compared with lacZ control cells (Fig. 5D). We speculate that the higher ratio of c-Myc phosphorylation at T58 to that at S62 may be attributed to higher activity of GSK3β and may contribute to GLIPR1-induced c-Myc downregulation. A different pattern was observed in LNCaP cells, in which the fraction of c-Myc phosphorylation at T58 in total c-Myc was increased ~3.1-fold, while c-Myc phosphorylation at S62 was increased ~4.6-fold in GLIPR1-expressing cells compared with lacZ-expressing cells (Fig. 5D). Thus, GLIPR1-stimulated c-Myc protein degradation may be related to GSK3β phosphorylation at T58 in DU145 cells, but not in LNCaP cells.

We thus hypothesized that CK1 participates in c-Myc protein degradation on the basis of the evidence of CK1 phosphorylation and destruction of dMyc in *Drosophila* (22) and the results from our cDNA microarray analysis (Fig. S5), western blot analyses (Fig. 4G) and immunofluorescence staining (Fig. 4H) that showed increased CK1α levels and marked redistribution of CK1α from Golgi complex into the cytoplasm in GLIPR1-induced prostate cancer cells. According to the consensus sequences of CK1 phosphorylation sites (T/S_pXXT/S_{CK1}) (27, 28) and reported phosphorylation sites on c-Myc protein (36), we

identified two potential sites on human c-Myc: S67 and S252 (Fig. 5C). To verify CK1α's involvement in GLIPR1-induced c-Myc protein degradation, we knocked down endogenous CK1α using specific siRNA and performed western blotting for c-Myc. Inhibition of CK1α largely restored c-Myc protein levels in both DU145 and LNCaP cells (Fig. 5E and 5F), indicating that CK1α participates in GLIPR1-induced c-Myc protein degradation. To further confirm that, we cotransfected LNCaP cells with c-myc and GLIPR1, GSK3β, or CK1α and analyzed their effects on c-Myc. We found that GLIPR1 expression and CK1α expression led to similarly reduced c-Myc protein, but GSK3β expression reduced c-Myc levels to a lesser extent (Fig. 5G).

To evaluate the significance of the GSK3β phosphorylation site at c-Myc T58 and the two potential CK1α phosphorylation sites at c-Myc S67 and S252 in GLIPR1-induced c-Myc degradation, we constructed three single point–mutation phosphorylation mutants by replacing GSK3β- or CK1α-targeted threonine or serine with alanine, and then cotransfected 293 cells with WT c-myc or mutant c-myc and GLIPR1 or control pcDNA empty vector. Fig. 6A shows that the T58A and S67A mutants had only a small effect on c-Myc protein levels relative to the WT c-Myc, whereas the S252A mutant effectively prevented GLIPR1-induced c-Myc protein degradation.

To verify the role of these phosphorylation sites in maintaining c-Myc protein stability, we expressed WT c-myc and mutant c-myc in DU145 cells and compared their protein stability after cycloheximide treatment. The WT c-Myc protein's half-life was 25 min, fairly close to the previously reported 30 min (37). The half-lives of the three phosphorylation mutants relative to that of WT c-Myc protein were as follows: T58A, two-fold increase; S67A, slightly increased; and S252A, greater than two-fold increase (70 min) (Fig. 6B).

Overall, our results reveal that a dual mechanism underlies GLIPR1's downregulation of c-Myc in PCa. In our proposed model (Fig. 6C), the initial step is GLIPR1's induction of CK1α expression and subcellular redistribution from the Golgi to the cytoplasm, where CK1α together with GSK3β phosphorylate β-catenin, leading to destruction of β-catenin. This primary mechanism leads to reduced active β-catenin and c-myc mRNA levels. In the second step, GLIPR1 promotes c-Myc protein degradation via GSK3β- and/or CK1α-mediated phosphorylation of c-Myc. This secondary mechanism generates recognition motif(s) for subsequent E3 ligase targeting and proteasome degradation of c-Myc. The resulting decrease in c-Myc activities leads to cell cycle arrest and inhibition of tumor growth. Importantly, the loss of *Glipr1* function and *c-myc* overexpression leads to premalignant phenotypic changes in vivo in mouse models.

Discussion

This study showed that (i) c-myc expression is inversely correlated with GLIPR1 expression and is positively correlated with GLIPR1 gene methylation in human PCa; (ii) *Glipr1* loss and c-myc overexpression have synergistic effects on induction of mPIN and PCa in mice; (iii) GLIPR1 suppresses *c-MYC* transcription by increasing CK1α expression and inducing CK1α redistribution in PCa cells, leading to cytoplasmic destruction of β-catenin and reduced β-catenin/TCF4-mediated *c-MYC* transcription; (iv) GSK3β and CK1α mediate GLIPR1-induced c-Myc protein degradation via c-Myc phosphorylation; (v) mutation of c-Myc S252, a consensus CK1 phosphorylation site, results in increased c-Myc protein stability, indicating phosphorylation of S252 on WT c-Myc plays an important role in GLIPR1-induced c-Myc ubiquitination and degradation. These findings extend our previously reported results that show *Glipr1*/*GLIPR1* is a direct p53 target gene with proapoptotic activities and tumor suppressor functions (1–3), and further underscores the importance of this tumor suppressor.

As we found in human PCa tissue samples *GLIPR1/Glipr1* loss is associated with gain of c-myc activities. This is not a simple inverse correlation but is mechanistically linked, i.e., loss of a gene that can effectively suppress c-myc mRNA and protein levels. As one of the most common oncogenes, c-myc represents an important therapeutic target. This study showed that the central mechanisms for GLIPR1 downregulation of c-myc is targeted destruction of β-catenin and c-Myc proteins. Together, these lead to dramatically reduced c-Myc protein levels.

Our ChIP assay results showing that GLIPR1 expression reduced TCF4 binding to the c-myc promoter, together with our results showing that GLIPR1 induced CK1α-mediated destruction of β-catenin, establish a mechanistic link between GLIPR1 and suppression of c-myc transcription. Over the last two decades aberrant β-catenin signaling was documented in many types of cancers, including PCa, and was associated with several important oncogenic signaling pathways, including Wnt (38–40). Phosphorylation of β-catenin S45 by CK1α is a well-documented crucial step leading to β-catenin destruction. We found that GLIPR1 can not only increase CK1α expression but also induce its dramatic redistribution from the Golgi to the cytoplasm, where it phosphorylates and thus promotes the destruction of β-catenin, thereby reducing c-myc transcription. To our knowledge, this is the first report of CK1α redistribution from the Golgi to the cytoplasm. In our opinion, this redistribution is critical to targeted destruction of both β-catenin and c-Myc.

Regulation of c-Myc protein degradation is an important mechanism underlying the precise control of this oncoprotein's cellular concentration. In this study, we identified a role for CK1α in regulating c-Myc protein's stability in experiments using CK1α siRNA and CK1α overexpression, validating our results in point-mutation experiments. In the 293 cell line, a point mutation at c-Myc S252 effectively abolished GLIPR1-induced c-Myc degradation; in DU145 cells, this point mutation markedly increased c-Myc protein stability. In contrast to GSK3β's well-documented role in c-Myc ubiquitination and degradation (15, 17–21), that of CK1 in those functions was previously reported only in *Drosophila*. Therefore, our results are the first evidence of CK1-mediated c-Myc ubiquitination and degradation in a mammalian system. This is also the first identification of c-Myc S252 as a key CK1 phosphorylation site that mediates c-Myc protein degradation. This finding of a role for CK1α in the regulation of c-Myc protein stability has special significance for PCa, given that Akt is deregulated in most PCa's, which in turn suppresses GSK3β, diminishing its role in the regulation of c-Myc protein stability.

GLIPR1's capacity for stimulating targeted destruction of oncogenic β-catenin and c-Myc holds promise for its use (in gene or protein applications) as a therapeutic agent for PCa and other malignancies in which β-catenin and c-myc expression is deregulated.

Supplementary Material

Refer to Web version on PubMed Central for supplementary material.

Acknowledgments

We thank Karen F. Phillips, ELS, for editing the manuscript.

Grant Support

This work was supported by grant R0150588 from the National Cancer Institute; by National Cancer Institute grant P50140388, the Prostate Cancer Specialized Program of Research Excellence at The University of Texas MD Anderson Cancer Center; and in part by the National Institutes of Health through MD Anderson's Cancer Center Support Grant, CA016672.

References

1. Li L, Abdel Fattah E, Cao G, Ren C, Yang G, Goltsov AA, et al. Glioma pathogenesis-related protein 1 exerts tumor suppressor activities through proapoptotic reactive oxygen species-c-Jun-NH2 kinase signaling. Cancer Res. 2008; 68:434–43. [PubMed: 18199537]
2. Ren C, Li L, Goltsov AA, Timme TL, Tahir SA, Wang J, et al. mRTVP-1, a novel p53 target gene with proapoptotic activities. Mol Cell Biol. 2002; 22:3345–57. [PubMed: 11971968]
3. Ren C, Li L, Yang G, Timme TL, Goltsov A, Ren C, et al. RTVP-1, a tumor suppressor inactivated by methylation in prostate cancer. Cancer Res. 2004; 64:969–76. [PubMed: 14871827]
4. Satoh T, Timme TL, Saika T, Ebara S, Yang G, Wang J, et al. Adenoviral vector-mediated mRTVP-1 gene therapy for prostate cancer. Hum Gene Ther. 2003; 14:91–101. [PubMed: 12614561]
5. Naruishi K, Timme TL, Kusaka N, Fujita T, Yang G, Goltsov A, et al. Adenoviral vector-mediated RTVP-1 gene-modified tumor cell-based vaccine suppresses the development of experimental prostate cancer. Cancer Gene Ther. 2006; 17:17.
6. Ren C, Ren CH, Li L, Goltsov AA, Thompson TC. Identification and characterization of RTVP1/GLIPR1-like genes, a novel p53 target gene cluster. Genomics. 2006; 88:163–72. [PubMed: 16714093]
7. Aytekin T, Ozaslan M, Cengiz B. Deletion mapping of chromosome region 12q13–24 in colorectal cancer. Cancer Genet Cytogenet. 2010; 201:32–8. [PubMed: 20633766]
8. Tam M, Lin P, Hu P, Lennon PA. Examining Hedgehog pathway genes GLI3, SHH, and PTCH1 and the p53 target GLIPR1/GLIPR1L1/GLIPR1L2 gene cluster using fluorescence in situ hybridization uncovers GLIPR1/GLIPR1L1/GLIPR1L2 deletion in 9% of patients with multiple myeloma. J Assoc Genet Technol. 2010; 36:111–4. [PubMed: 20978342]
9. Rosenzweig T, Ziv-Av A, Xiang C, Lu W, Cazacu S, Taler D, et al. Related to testes-specific, vespid, and pathogenesis protein-1 (RTVP-1) is overexpressed in gliomas and regulates the growth, survival, and invasion of glioma cells. Cancer Res. 2006; 66:4139–48. [PubMed: 16618735]
10. Nesbit CE, Tersak JM, Prochownik EV. MYC oncogenes and human neoplastic disease. Oncogene. 1999; 18:3004–16. [PubMed: 10378696]
11. Junttila MR, Westermarck J. Mechanisms of MYC stabilization in human malignancies. Cell Cycle. 2008; 7:592–6. [PubMed: 18256542]
12. Meyer N, Penn LZ. Reflecting on 25 years with MYC. Nat Rev Cancer. 2008; 8:976–90. [PubMed: 19029958]
13. Wierstra I, Alves J. The c-myc promoter: still MysterY and challenge. Adv Cancer Res. 2008; 99:113–333. [PubMed: 18037408]
14. Liu J, Levens D. Making myc. Curr Top Microbiol Immunol. 2006; 302:1–32. [PubMed: 16620023]
15. Arnold HK, Zhang X, Daniel CJ, Tibbitts D, Escamilla-Powers J, Farrell A, et al. The Axin1 scaffold protein promotes formation of a degradation complex for c-Myc. EMBO J. 2009; 28:500–12. [PubMed: 19131971]
16. Sears R, Leone G, DeGregori J, Nevins JR. Ras enhances Myc protein stability. Mol Cell. 1999; 3:169–79. [PubMed: 10078200]
17. Sears RC. The life cycle of C-myc: from synthesis to degradation. Cell Cycle. 2004; 3:1133–7. [PubMed: 15467447]
18. Yeh E, Cunningham M, Arnold H, Chasse D, Monteith T, Ivaldi G, et al. A signalling pathway controlling c-Myc degradation that impacts oncogenic transformation of human cells. Nat Cell Biol. 2004; 6:308–18. [PubMed: 15048125]
19. Welcker M, Clurman BE. FBW7 ubiquitin ligase: a tumour suppressor at the crossroads of cell division, growth and differentiation. Nat Rev Cancer. 2008; 8:83–93. [PubMed: 18094723]
20. Welcker M, Orian A, Jin J, Grim JE, Harper JW, Eisenman RN, et al. The Fbw7 tumor suppressor regulates glycogen synthase kinase 3 phosphorylation-dependent c-Myc protein degradation. Proc Natl Acad Sci U S A. 2004; 101:9085–90. [PubMed: 15150404]

21. Sears R, Nuckolls F, Haura E, Taya Y, Tamai K, Nevins JR. Multiple Ras-dependent phosphorylation pathways regulate Myc protein stability. Genes Dev. 2000; 14:2501–14. [PubMed: 11018017]
22. Galletti M, Riccardo S, Parisi F, Lora C, Saqcena MK, Rivas L, et al. Identification of domains responsible for ubiquitin-dependent degradation of dMyc by glycogen synthase kinase 3beta and casein kinase 1 kinases. Mol Cell Biol. 2009; 29:3424–34. [PubMed: 19364825]
23. Siddall NA, Lin JI, Hime GR, Quinn LM. Myc--what we have learned from flies. Curr Drug Targets. 2009; 10:590–601. [PubMed: 19601763]
24. Xu C, Kim NG, Gumbiner BM. Regulation of protein stability by GSK3 mediated phosphorylation. Cell Cycle. 2009; 8:4032–9. [PubMed: 19923896]
25. Wu D, Pan W. GSK3: a multifaceted kinase in Wnt signaling. Trends Biochem Sci. 2009; 35:161–8. [PubMed: 19884009]
26. Taelman VF, Dobrowolski R, Plouhinec JL, Fuentealba LC, Vorwald PP, Gumper I, et al. Wnt signaling requires sequestration of glycogen synthase kinase 3 inside multivesicular endosomes. Cell. 143:1136–48. [PubMed: 21183076]
27. Knippschild U, Gocht A, Wolff S, Huber N, Lohler J, Stoter M. The casein kinase 1 family: participation in multiple cellular processes in eukaryotes. Cell Signal. 2005; 17:675–89. [PubMed: 15722192]
28. Price MA. CKI, there's more than one: casein kinase I family members in Wnt and Hedgehog signaling. Genes Dev. 2006; 20:399–410. [PubMed: 16481469]
29. Liu C, Li Y, Semenov M, Han C, Baeg GH, Tan Y, et al. Control of beta-catenin phosphorylation/degradation by a dual-kinase mechanism. Cell. 2002; 108:837–47. [PubMed: 11955436]
30. Thorne CA, Hanson AJ, Schneider J, Tahinci E, Orton D, Cselenyi CS, et al. Small-molecule inhibition of Wnt signaling through activation of casein kinase 1alpha. Nat Chem Biol. 2010; 6:829–36. [PubMed: 20890287]
31. Price MA, Kalderon D. Proteolysis of the Hedgehog signaling effector Cubitus interruptus requires phosphorylation by Glycogen Synthase Kinase 3 and Casein Kinase 1. Cell. 2002; 108:823–35. [PubMed: 11955435]
32. Kim S, Park Y, Park ES, Cho JY, Izzo JG, Zhang D, et al. Prognostic Biokarmers for Esophageal Adenocarcinoma Identified by Analysis of Tumor Transcriptome. PLoS One. 2010; 5:e15074. [PubMed: 21152079]
33. Gurel B, Iwata T, Koh CM, Jenkins RB, Lan F, Van Dang C, et al. Nuclear MYC protein overexpression is an early alteration in human prostate carcinogenesis. Mod Pathol. 2008; 21:1156–67. [PubMed: 18567993]
34. Yang G, Timme TL, Frolov A, Wheeler TM, Thompson TC. Combined c-Myc and caveolin-1 expression in human prostate carcinoma predicts prostate carcinoma progression. Cancer. 2005; 103:1186–94. [PubMed: 15712208]
35. MacDonald BT, Tamai K, He X. Wnt/beta-catenin signaling: components, mechanisms, and diseases. Dev Cell. 2009; 17:9–26. [PubMed: 19619488]
36. cited; Available from: http://www.phosphosite.org/proteinAction.do?id=947.
37. Ramsay G, Evan GI, Bishop JM. The protein encoded by the human proto-oncogene c-myc. Proc Natl Acad Sci U S A. 1984; 81:7742–6. [PubMed: 6393124]
38. Polakis P. Wnt signaling and cancer. Genes Dev. 2000; 14:1837–51. [PubMed: 10921899]
39. Robinson DR, Zylstra CR, Williams BO. Wnt signaling and prostate cancer. Curr Drug Targets. 2008; 9:571–80. [PubMed: 18673243]
40. Takemaru KI, Ohmitsu M, Li FQ. An oncogenic hub: beta-catenin as a molecular target for cancer therapeutics. Handb Exp Pharmacol. 2008:261–84. [PubMed: 18491056]

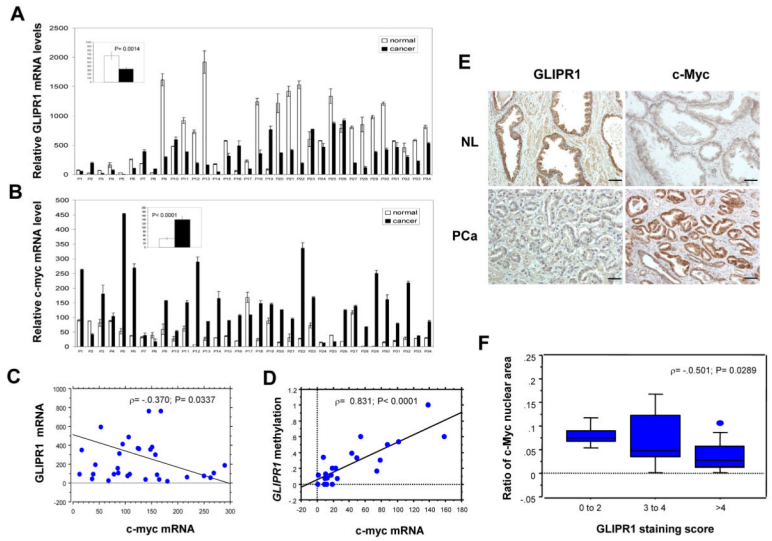

Figure 1.

GLIPR1 expression and c-Myc expression are inversely correlated in human prostate cancer tissue samples. A and B, Graphs show results of qRT-PCR analysis of GLIPR1 and c-myc mRNA levels in 34 pairs of PCa tissues and adjacent normal prostate tissues. Inserts summarize the paired *t* test results for the comparison of GLIPR1 and c-myc mRNA expression between PCa tissues and adjacent normal prostate tissues. C, Correlation analysis of GLIPR1 and c-myc mRNA expression. D, Correlation analysis of the methylation of GLIPR1 promoter and c-myc mRNA expression. E. Representative immunohistochemically stained slides show GLIPR1 and c-Myc protein levels in normal prostate (NL) and PCa tissues. Bars= 100 μm. F, Box plots of c-Myc nuclear immunostaining versus GLIPR1 staining score in human PCa tissue specimens. Error bars indicate SD.

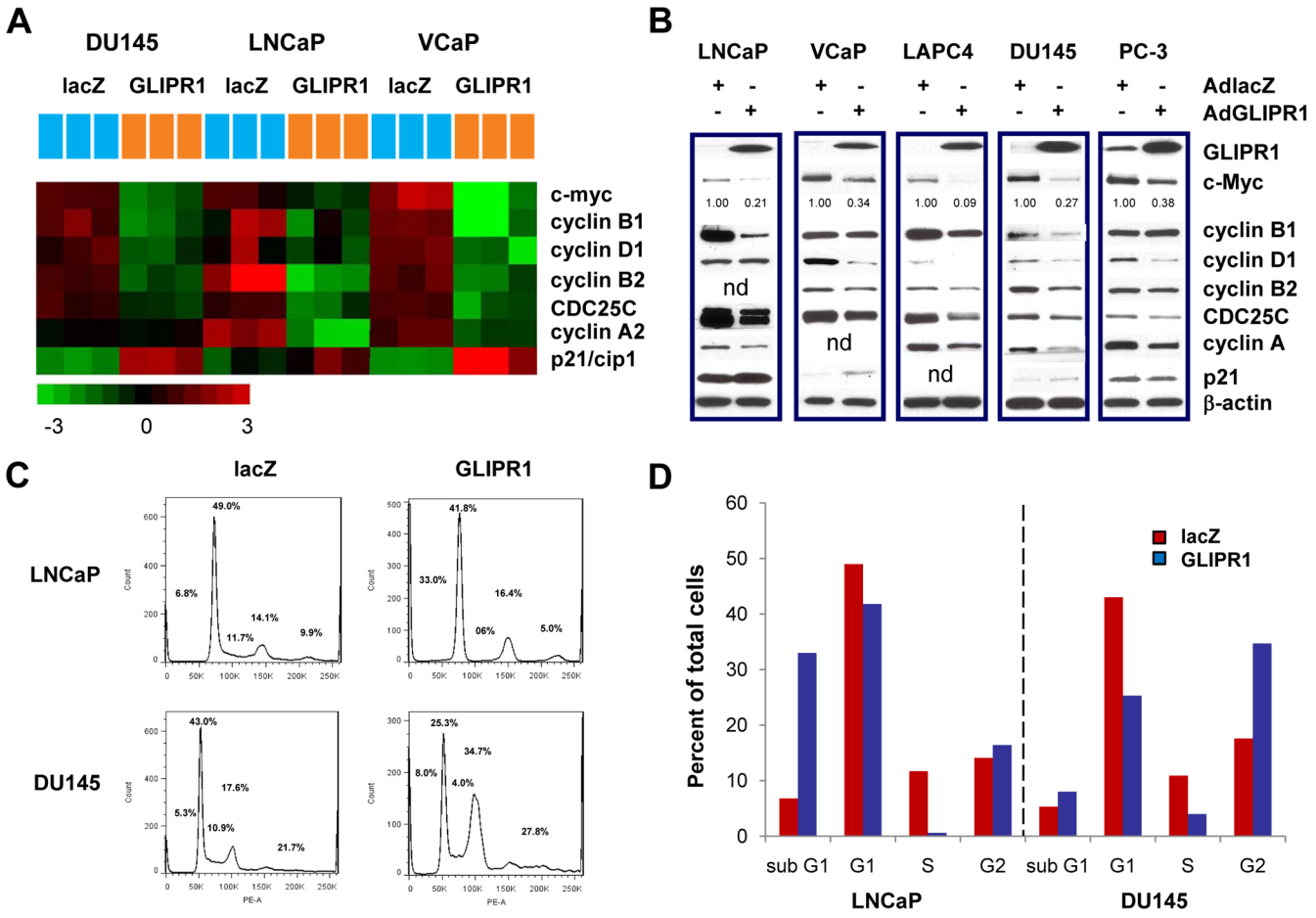

Figure 2.

GLIPR1 restoration in prostate cancer cells leads to c-Myc downregulation and cell cycle inhibition. A, cDNA microarray heat map summarizes the downregulation of c-myc; cyclins B1, D1, B2, and A2; and CDC25C and the upregulation of the cell cycle inhibitor p21 in the prostate cancer (PCa) cell lines. B, Western blot analysis. nd = not detectable. C and D, Cell cycle distribution in GLIPR1 restored LNCaP and DU145 PCa cells.

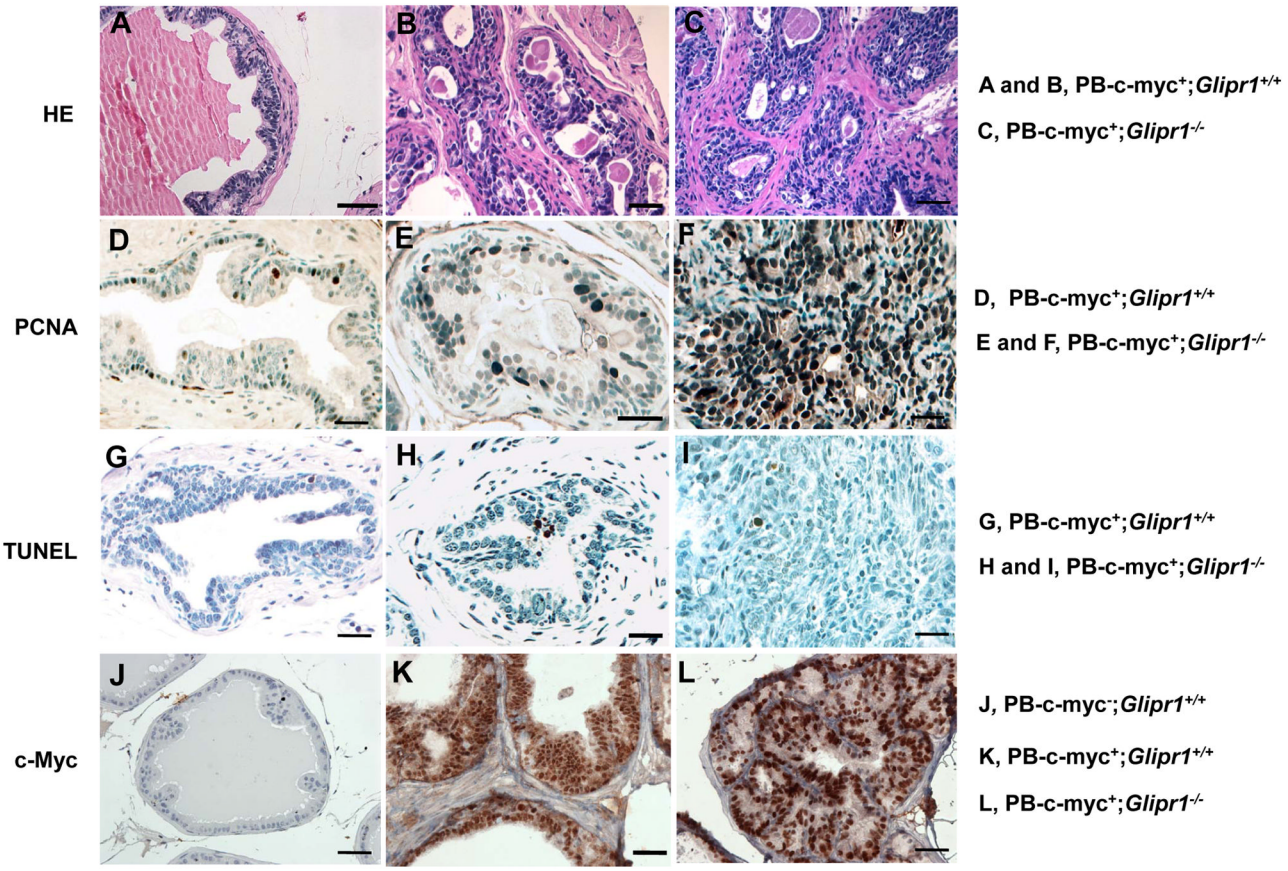

Figure 3.

Immunohistochemical analysis of prostate tissue sections from bigenic mice. A-C, Hematoxylin and eosin (HE)-stained sections show hyperplastic glandular epithelium (with atypia) (A), prostatic intraepithelial neoplasm (mPIN) (B) and carcinoma (C). D-F, PCNA labeling. G-I, TUNEL assay. J–L, c-Myc immunostaining results in normal glandular prostatic epithelial tissue (J) and in mPIN tissues (K and L).

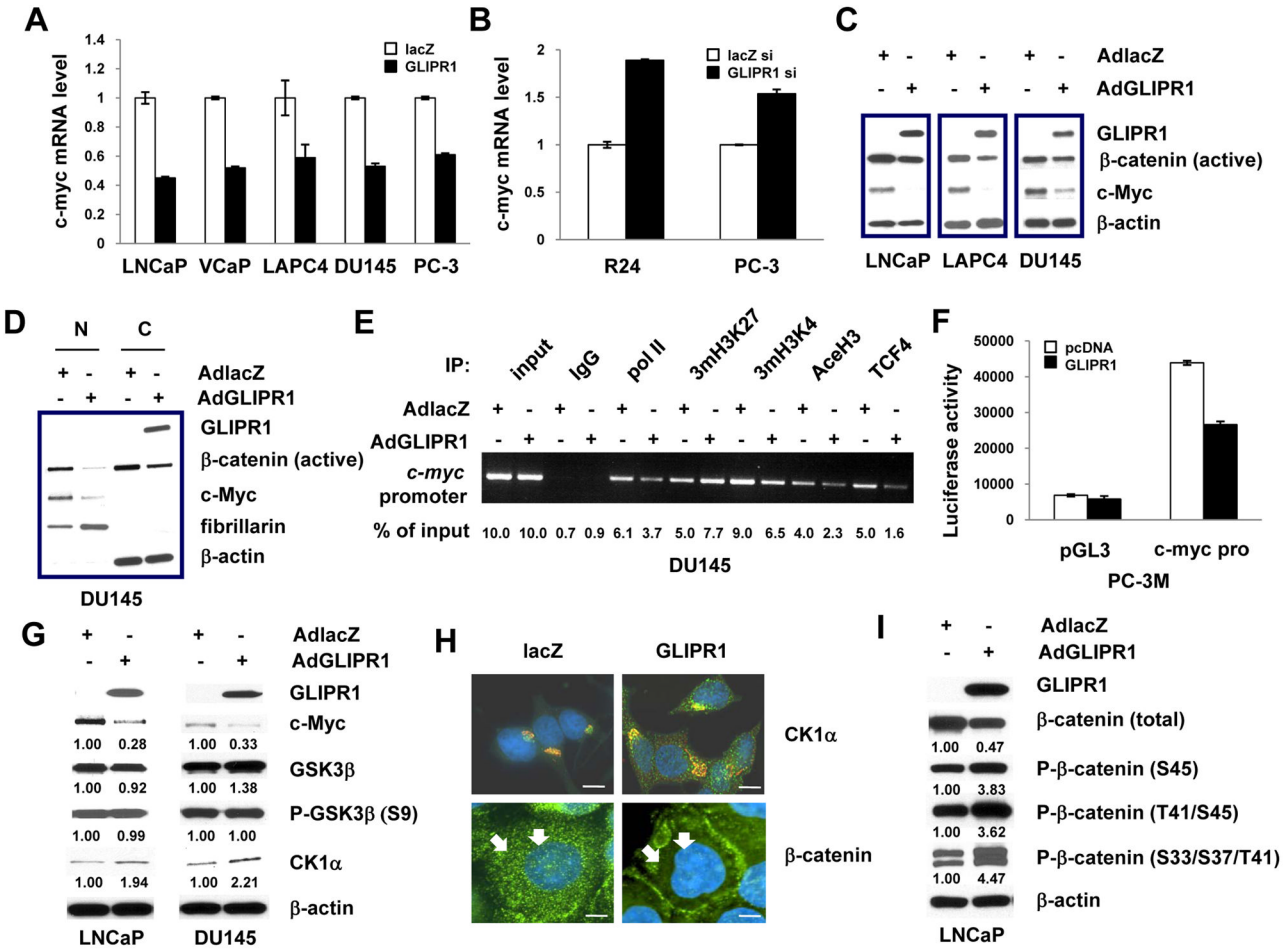

Figure 4.

GLIPR1 negatively regulates *c-myc* promoter activities. A and B, qRT-PCR analysis showed c-myc mRNA levels in GLIPR1-enforced (A) and GLIPR1-knocked down (B) PCa cell lines. C, Western blotting analysis for cellular β-catenin and c-Myc proteins. D, Subcellular fractionation for nuclear (N) and cytosolic (C) β-catenin and c-Myc. Fibrillarin and β-actin were used as loading controls for N and C fractions, respectively. E, ChIP assay. Pol II= RNA polymerase II; 3mH3K27= trimethyl-histone H3 (Lys27); 3mH3K4= trimethyl-histone H3 (Lys4); AceH3= acetyl-histone H3 (Lys27). F, Luciferase reporter assay. G, Western blotting results show the protein expression levels of GSK3β, P-GSK3β (S9), and CK1α in LNCaP and DU145 cells. H, Representative immunofluorescence images for subcellular distribution of CK1α and β-catenin in GLIPR1 or lacZ-expressed PCa cells. Bars= 10 μm (top) or 5 μm (bottom). I, Western blotting results show β-catenin phosphorylation in GLIPR1-expressed LNCaP cells. Error bars indicate SD.

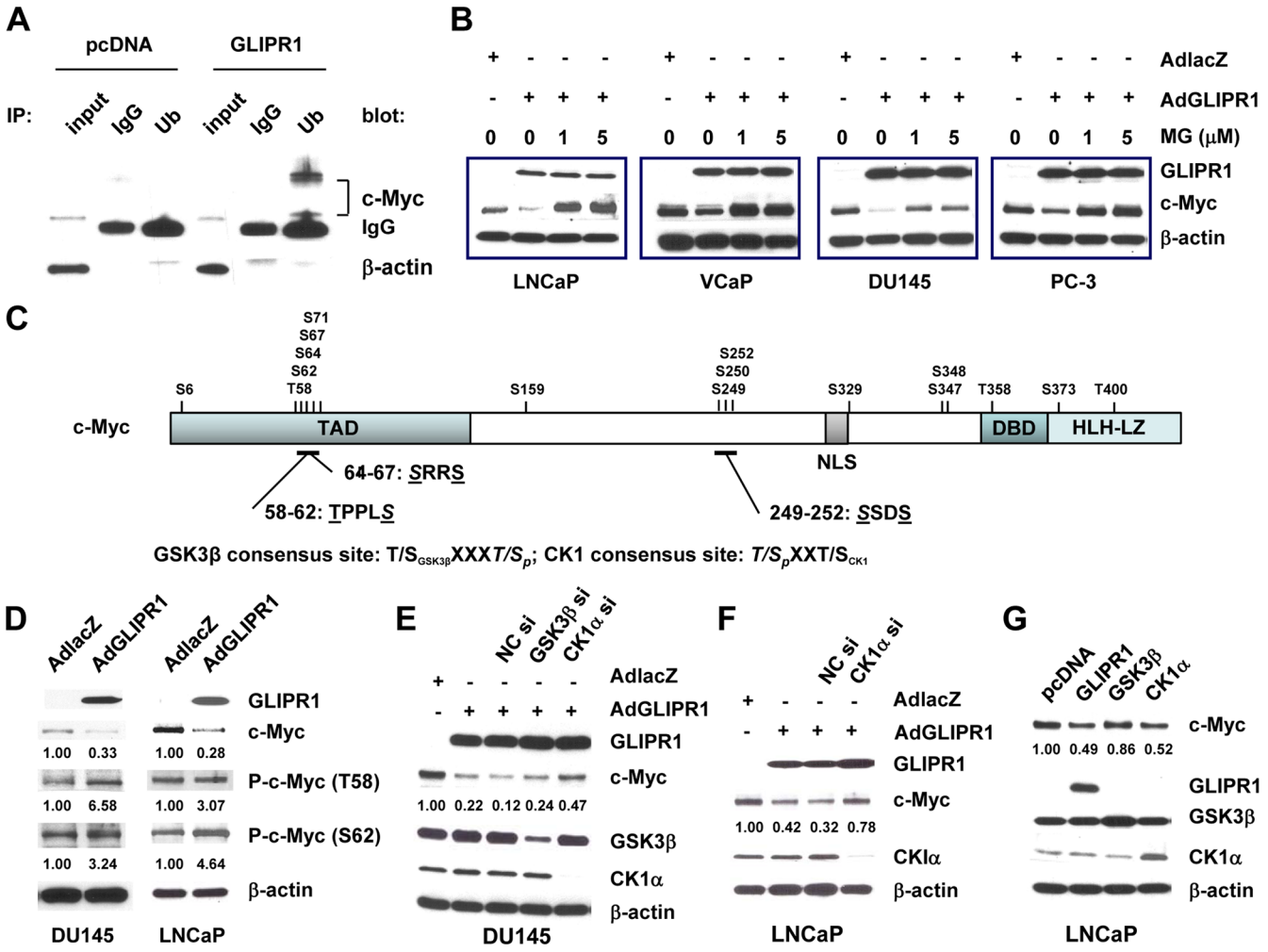

Figure 5.

GLIPR1-induced c-Myc downregulation involves ubiquitination, proteasome degradation, and CK1α. A, Immunoprecipitation (IP) analysis of ubiquitinated c-Myc in GLIPR1-expressing cells. B, Blots depict that proteasome inhibitor MG132 (MG) abrogates GLIPR1-induced c-Myc protein degradation in PCa cells. C, Diagram illustrates the reported phosphorylated serine (S)/threonine (T) and potential CK1 phosphorylation sites on the c-Myc protein molecule. Underlined letters are phosphorylation sites and italicized letter indicate priming phosphorylation sites. D, Western blots show c-Myc, P-c-Myc (T58), and P-c-Myc (S62) protein levels in GLIPR1-overexpressed DU145 and LNCaP cells. E and F, Western blotting indicated that suppressing endogenous GSK3β or CK1α expression with siRNA in GLIPR1-overexpressed DU145 (E) and LNCaP (F) cells partially restored the level of c-Myc protein. NC= negative control. G, Transfection of LNCaP cells with GSK3 β and CK1α reduced the level of c-Myc protein.

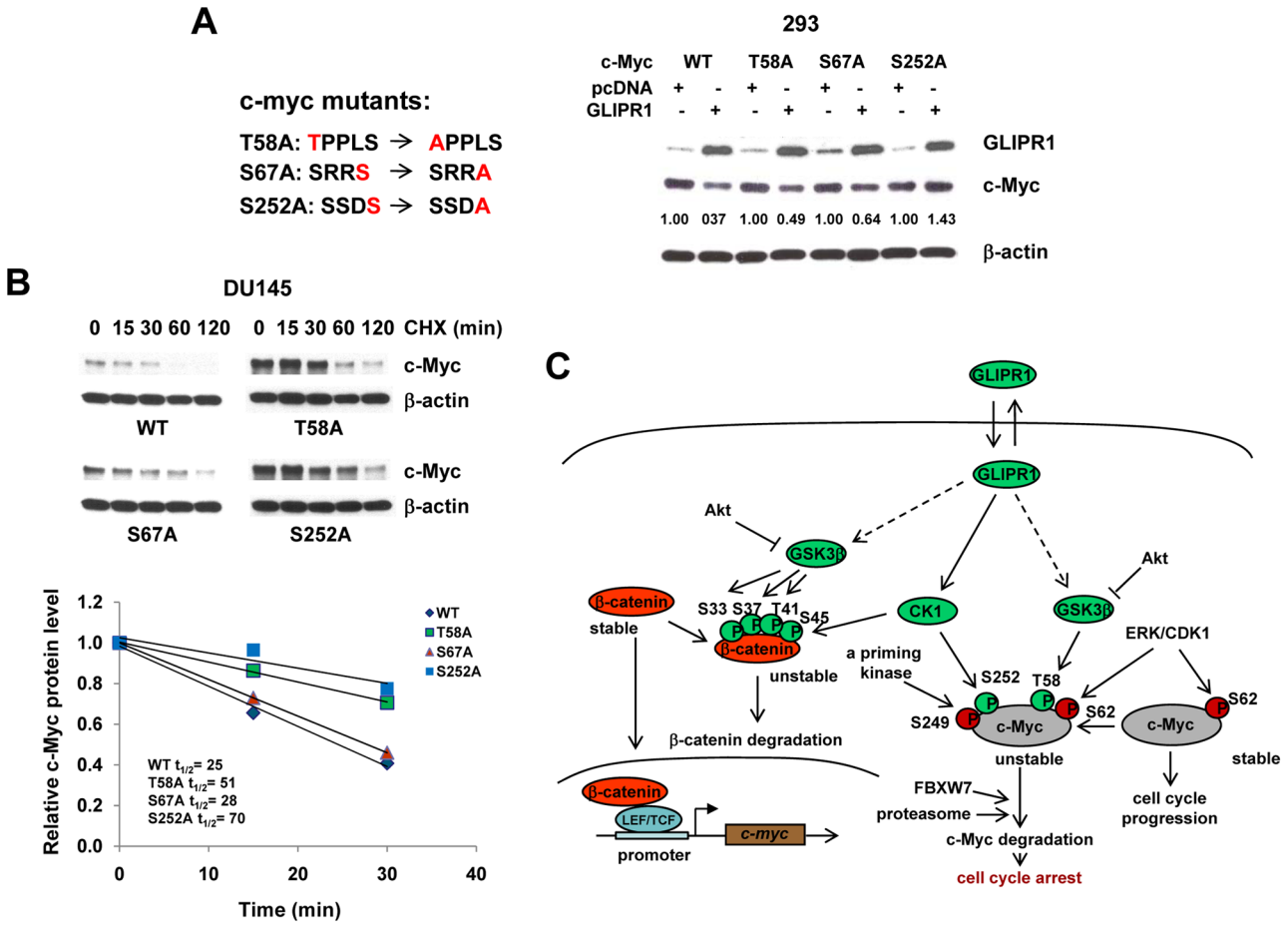

Figure 6.

Phosphorylation of c-Myc on S252 is important in GLIPR1-induced destruction of c-Myc protein. A, Three phosphorylation site point-mutation mutants (left panel) were generated by replacing GSK3β- and CK1α-targeted threonine (T) and serine (S) with alanine (A) at the indicated positions (in red). Western blots (right panel) show the resulting c-Myc protein levels after cotransfection of 293 cells with wild-type (wt) or mutant c-myc and GLIPR1 or pcDNA. B, DU145 prostate cancer cells were transfected with wt or mutant c-Myc and then treated with cycloheximide (CHX) for the indicated times, followed by (top panel) western blot analysis and (bottom panel) quantitative analysis for c-Myc protein stability. $t_{1/2}$ = half-life. C, Diagram illustrates our proposed model of GLIPR1-induced molecular signaling.

Table 1

Synergistic effects of c-Myc overexpression and loss of *Glipr1* function results in significantly increased mPIN and leads to prostate cancer.

Animal Group		Type and Frequency of Lesions*		
***c-myc* Transgene Status**	***Glipr1* Status**	**Epithelial Hyperplasia (with Atypia)**	**mPIN**	**Carcinoma**
PB-c-myc^{-}	*Glipr1*$^{+/+}$	2/13	0/13	0/13
PB-c-myc^{-}	*Glipr1*$^{-/-}$	4/25	6/25	0/25
PB-c-myc^{+}	*Glipr1*$^{+/+}$	10/48	11/48	0/48
PB-c-myc^{+}	*Glipr1*$^{-/-}$	15/49	23/49*	3/49

*p = 0.023 versus PB-c-myc^{+};*Glipr1*$^{+/+}$ mice and p = 0.0011 versus PB-c-myc^{-};*Glipr1*$^{+/+}$ mice; Fisher's exact test.